TECHNICAL MEMORANDUMS

NATIONAL ADVISORY COMMITTEE FOR AERONAUTICS

No. 809

TESTS FOR THE DETERMINATION OF THE STRESS CONDITION IN TENSION FIELDS

By R. Lahde and H. Wagner

Luftfahrtforschung
Vol. 13, No. 8, August 20, 1936
Verlag von R. Oldenbourg, München und Berlin

Washington
November 1936

NATIONAL ADVISORY COMMITTEE FOR AERONAUTICS

TECHNICAL MEMORANDUM NO. 809

TESTS FOR THE DETERMINATION OF THE STRESS CONDITION IN TENSION FIELDS*

By R. Lahde and H. Wagner

SUMMARY

By "tension field" is meant the thin-walled web plate of a sheet-metal girder which buckles under the effect of a transverse force as a result of forming oblique wrinkles.

The tension-field theory (reference 1) makes it possible to calculate the principal tension in magnitude and direction in the web plate, as well as the stress in the uprights and flanges while disregarding the flexural resistance of the web plate. The tension-field theory treats the extreme case of very greatly (∞) exceeded buckling load of the web plate.

The present experiments treat the stress of actual tension fields within the elastic range. They give the magnitude of the flexural stresses due to wrinkling. They also disclose, particularly by slightly exceeded buckling load, the marked unloading - as compared with the tension-field theory - of the uprights as a result of the flexural stiffness of the web plate.

As regards the experimental set-up and interpretation of the tests, the present report forms a supplement to the previously published experiments for the determination of the effective width of bulged sheets (reference 2). The test sheets were again clamped at the edges and brought to buckling through shearing and compressive stresses applied in the direction of the long sides.

---

*"Versuche zur Ermittlung des Spannungszustandes in Zugfeldern." Luftfahrtforschung, vol. 13, no. 8, August 20, 1936, pp. 262-268.

INTRODUCTION

Consider a plate girder consisting of two flanges, a thin-walled smooth web plate, and stiffening sections or, as they are also called, uprights (fig. 1). Clamping the girder at one end and applying a small transverse force Q at the other end, subjects the sheet to a shearing stress. If Q is further increased, the sheet develops oblique wrinkles in whose direction the sheet is stressed in tension. The tension-field theory treats this stress condition without allowance for the flexural stiffness of the web plate; this corresponds to the extreme case of an infinitely exceeded buckling load.

The following is an account of the test data of the stress condition in such tension fields.

The stress condition is largely dependent on the ratio of the applied transverse force to that transverse force at which wrinkling commences. As regards the stress in the sheet the experiments disclosed, above everything else, the appearance of flexural stresses due to wrinkling which are not qualitatively accounted for by the tension-field theory. By greatly exceeded buckling load they lead to high stress values, especially at the edge where the fixation has forced the sheet into the plane. As regards the stress of the neutral axis of the sheet free from flexural stresses, good agreement is obtained with the values computed from the tension-field theory, especially when the buckling load has been little exceeded.

The compressive stresses in the uprights were also experimentally defined. Here it revealed - notably, by slightly exceeded buckling load - a substantial unloading, compared to the theoretical values, which is attributable to the effective support of the sheet by virtue of its flexural stiffness.

The flange stresses in compression and bending, as well as the angle of displacement, and the shear stiffness were equally determined. These quantities always range between two extremes: the values from the tension-field theory on the one hand, and those valid for the buckling resistant sheet on the other hand. Discounting the shearing stiffness, an increasing overstepping of the buckling load is consistently followed by a steady change of the values for the buckling resistant sheet to tension-field

values, which can be represented as asymptotes to the experimental curves.

The experimental quantities are given in nondimensional form (reference 2, p. 223) for reasons of the general validity of the test data.

As independent variables, the terms

$$\frac{\tau}{E}\left(\frac{t}{s}\right)^2 \quad \text{and} \quad \frac{\sigma_p}{\tau}$$

were chosen, whereby

σ_p is compression in upright

E, Young's modulus

s, sheet thickness

$\tau = \frac{Q}{h\,s}$, shearing stress of sheet

Conformable to the formula for the buckling load of a flat sheet in shear,

$$\tau_k = \kappa\, E \left(\frac{s}{t}\right)^2$$

the value $\frac{\tau}{E}\left(\frac{t}{s}\right)^2$ may be considered as a measure for the degree of exceeded buckling load.

As regards the employed test and interpretation method, the present experiments are largely in accord with the report "tests for the determination of the effective width of bulged sheets" (reference 2, p. 223).

RESULTS

To provide a better understanding of the test data, the prccesses involved in the loading of a plate girder are once more briefly analyzed. When the plate girder shown in figure 1 is slightly stressed by a transverse force Q, the sheet itself is stressed in shear.

If Q is increased, the sheet collapses under a certain shearing stress τ_k (critical shearing stress). If Q continues to increase the sheet develops - additive to $\tau = \frac{Q}{h\,s}$ - progressively increasing tension stresses σ_y in beam direction, and σ_x in direction of the uprights* (fig. 2). This stress condition σ_x, σ_y, τ is identical with the oblique principal stresses σ and σ_q shown in figure 2. The tension-field theory which ignores the flexural stiffness of the sheet, yields $\sigma_q = 0$; that is, a single axial stress attitude σ, whose direction is at the same time the direction of the wrinkles. The tension stresses acting in the direction of the uprights, tend to bring the flanges closer together, since the sheet is solidly riveted at the flanges. The result is that the uprights joining the flanges are compressed and become shorter. At the junction point of sheet and upright, where buckling is prevented, the sheet undergoes in the direction of the uprights, the same contraction and (discounting the slight deflection due to transverse contraction) the same compressive stress as the upright, resulting in a stress distribution somewhat on the order of figure 3. The compression in the upright and in the adjacent parts of the sheet is in equilibrium with the tension forces in the sheet at the flange.

Consider now a girder with a smaller cross-sectional area of the uprights than in the previously analyzed case, the loads and dimensions to be the same as before. Now the uprights undergo a higher stress and consequently a greater compression. This increase, howver, does not take place in the same ratio as the sectional reduction because the stress condition in the sheet is now different: Conformable to the greater compression of the uprights, the compressive stress of the sheet has become greater at the upright; the sheet now takes up more compression. The parts of the sheet lying more in the center between the uprights are also affected; their tensile stress becomes less. As a result of this, the compression to be taken up by the upright becomes less, inasmuch as it holds the equilibrium of the sheet forces at the flange.

These considerations reveal that the compressive stress in the upright depends upon the shearing stress but further also, on the sectional area of the upright.

---

*The longitudinal stresses due to the bending of the whole girder, are discounted here.

STRESS IN UPRIGHTS

Figure 4 illustrates this relationship as evolved from the experiments. The particular method of representation was chosen with a view to the most frequently encountered practical case, namely, to find the necessary area F_p of the upright giving for otherwise predetermined s, t, and τ a certain required compressive stress σ_p in the uprights.

The graph discloses that even in the event of fairly far exceeded buckling load in shear (buckling starts at $\frac{\tau k_o}{E}\left(\frac{t}{s}\right)^2 = 7.8$) the compressive stress σ_p in the upright is still considerably less than the figures (asymptotes) from the tension-field theory.

By slightly exceeded buckling load in shear, the marked support of the sheet will in many cases make it impossible to attain a requisite compressive stress in the uprights; then F_p/st either becomes equal to zero or negative.

STRESS IN THE SHEET

The stress in the sheet consists of the previously described stress condition σ_x, σ_y, τ and the flexural stresses due to wrinkling.* The stress condition σ_x, σ_y, τ represents the mean values of the stresses over the sheet thickness, which are equal to the stresses in the area midway between the two sheet surfaces - the median area. The stress σ_{id} in the median area, evolved on the basis of these strains, is shown in figure 6.** Even by very small

---

*The energy of form change giving the value

$$\sigma_{id} = \sqrt{(\sigma_x - \sigma_y)^2 + \sigma_x \sigma_y + 3\tau^2}$$

for a plain stress condition as ideal stress (i.e., that single axial stress of equal form-change energy) was considered as decisive for the stress.

**This σ_{id} is as yet dependent on the coordinates x and y; here the mean σ_{id} of the sheet strip midway between two uprights was plotted.

values of $\frac{\tau}{E}\left(\frac{t}{s}\right)^2$ the results here deviate very little from the values shown at the right-hand side, computed as single axial tension stresses in the tension-field theory and amounting to about 2τ.* The cumulative bending stresses result in still higher stresses in the outside fibers of the sheet. The resultant stress in the outside fiber has at small $\frac{\tau}{E}\left(\frac{t}{s}\right)^2$ a maximum value midway between two uprights (fig. 6). They drop again at large $\frac{\tau}{E}\left(\frac{t}{s}\right)^2$ and asymptotically approach the values from the tension-field theory.

Accordingly, there is in normal cases (that is, when $\frac{\sigma_p}{\tau} \approx 1$) a 60- to 70-percent overstress as against the stress 2τ from the tension-field theory.

When $\frac{\tau}{E}\left(\frac{t}{s}\right)^2$ rises above about 300, the maximum overstress takes place more toward the sheet edge, where the fixation of edge sections forces the wrinkles in the plane. The few available test points reveal considerable scattering, whence no attempt was made to plot them in curves. But even so, the experiments proved that the stresses here, in contrast to the σ_{id} in the center are still fairly high even at very great values of $\frac{\tau}{E}\left(\frac{t}{s}\right)^2$. The highest stresses recorded amounted to $4.5\,\tau$; and it is recommended to figure with this value for great values of $\frac{\tau}{E}\left(\frac{t}{s}\right)^2$.

As regards the sheet dimensions, it should perhaps be added that the rise of σ_{id} at the edge is chiefly due to the flexural stresses caused by wrinkling. As to the reaching of the yield point, the usually somewhat higher yield point in the outside fiber of the sheet is then decisive. A certain overstepping of the yield point through

---

*In this representation the plotting of the test curves was omitted in view of the difficulties as a result of the close bunching and partial overlapping of the experimental points. Moreover, the stresses are quite accurately illustrated through the tension-field theory, as seen from the position of the test points.

these flexural stresses under operating load, is not serious even when the transverse forces are always applied in the same sense of direction (i.e., always produce the same wrinkling again), and when this maximum load occurs or disappears only rarely. Then the first maximum load occurrence produces a prestress condition in the sheet, which prevents a subsequent overstepping of the yield point.

Since this overstepping of the yield point at the edge is restricted to a small locally confined zone, it practically produces no change in the stress attitude of the sheet and the test data retain their validity in this case. It is only when the σ_{id} in the center exceeds the yield point that discrepancies from the test data given here occur. Then the stress attitude approaches that of the tension-field theory, and by substantial overstepping of the yield point, all the stresses are more exactly computable, according to tension-field theory.

CUMULATIVE FLANGE STRESSES

Axial Loads

The buckled sheet discloses in the y-direction tensile stresses which, for reasons of equilibrium, induce cumulative axial stresses in the flanges. Figure 7 illustrates the ratio of the axial flange stress H to transverse force Q plotted against $\frac{\tau}{E}\left(\frac{t}{s}\right)^2$ for several values of $\frac{\sigma_p}{\tau}$, with the tension-field data at the right-hand side.

Bending Moments

The stresses $\overline{\sigma_x}$ in the x-direction, produce bending stresses in the flanges. The bending moments M were calculated from the measured $\overline{\sigma_x}$ over width t. Figure 8 gives the values $\frac{M}{\tau\ s\ t^2}$ against $\frac{\tau}{E}\left(\frac{t}{s}\right)^2$ and $\frac{\sigma_p}{\tau}$.

ANGLE OF DISPLACEMENT AND STIFFNESS IN SHEAR

The formulas for computing the angle of displacement or angle of torsion of hollow bodies always contain the shear modulus G of the material as $G = \tau/\gamma$. If it in-

volves thin-walled plate girders or hollow bodies built up of thin sheet, then in conformity to the greater angle of displacement, a value smaller than $\frac{\tau}{\gamma} = G$ must replace G in the particular formula. Figure 9 gives this ratio τ/γ of the buckled sheet to the elasticity modulus of the particular material versus $\frac{s}{t\sqrt{\frac{\tau}{E}}}$ and $\frac{\sigma_p}{\tau}$.

In the chosen method of plotting, the value $\frac{\tau/E}{\gamma}$ drops linearly from the value 0.385 (theoretical value of nonbuckled sheet at $\nu = 0.3$) to the value of the tension-field theory which is reached at $\frac{s}{t\sqrt{\frac{\tau}{E}}} = 0$.

If it pertains to the torsional stiffness of hollow bodies, as against vibrations, for instance, the derivative $\partial\tau/\partial\gamma$ substitutes for the shear modulus (fig. 10). This value was obtained by differentiation of the experimental values. The plotted point represents the stiffness of the nonbuckled sheet which is equal to the shear modulus. On buckling, the stiffness drops suddenly to a lesser value, whence it continues to drop almost linearly until it reaches at $\frac{s}{t\sqrt{\frac{\tau}{E}}} = 0$ the values from the tension-field theory; in this case, equal to τ/γ.

We also investigated the shear stiffness of plate walls made to buckle under compressive stresses applied only in the direction of the long edges (fig. 11). It is dependent on the compressive stress σ_p in the edge section; it decreases as σ_p increases. In view of these experiments, it appears that in the extreme case of infinite exceeding of the compression buckling load, the stiffness becomes equal to zero.

SAMPLE PROBLEM

Determine the dimensions of a flat part of the side wall of duralumin shell body having the following characteristics: spacing of stringers, h = 50 cm; spacing of uprights, t = 20 cm; shear flow, τ s = 60 kg/cm.

The admissible shearing stress is estimated at τ = 1,000 kg/cm^2; so that $s = 0.06$ cm and $\frac{\tau}{E}\left(\frac{t}{s}\right)^2 = 159$.

We also assess $\frac{\sigma_p}{\tau} = 1$, so that (fig. 4) $F_p = 0.19 \times 0.06 \times 20 = 0.23$ cm^2.

In the absence of better data, we approximate the necessary buckling stiffness of the uprights according to the tension-field theory (reference 1, pp. 228 and 260). This seems justified because in this particular case the buckling-shearing stress = $7.8\ E\ (s/t)^2$ is already materially exceeded:

$$\frac{\tau}{\tau_k} = \frac{\frac{\tau}{E}\left(\frac{t}{s}\right)^2}{\frac{\tau_k}{E}\left(\frac{t}{s}\right)^2} = \frac{159}{7.8} = 20.4$$

In the tension field the force in the upright would be:

$$V_{th} \approx 0.9\ Q\ \frac{t}{h} = 1{,}080 \text{ kg}$$

The value $\frac{t}{h \cot \alpha}$ is certainly less than 0.5; so that $\frac{V_{th}}{P_E} = 5$ may be assumed. This makes the requisite inertia moment:

$$I = \frac{V_{th}\ h^2}{\frac{V_{th}}{P_E}\ \pi^2\ E} = 0.0785 \text{ cm}^4$$

The uprights were U sections as shown in figure 12. The stress condition in the tension field is governed by the compressive stress of the fiber of the section lying at the skin. Because of the eccentricity e_1 the cross-sectional area to be calculated is therefore not the actual section F_p but rather a reduced cross-sectional area corresponding to the expression:

$$F_{p \text{ reduced}} = \frac{F_{pw}}{1 + \left(\frac{e_1}{i}\right)^2}$$

Then $F_{p\ reduced} = 0.23\ cm^2$, and the actual cross-sectional area becomes

$$F_{pw} = 2\ F_{reduced} = 0.46\ cm^2$$

Thus, suppose $a = 1.5$ cm, then $s_p = \frac{0.46}{3.5 \times 1.5} = 0.09$ cm, and the inertia moment is:

$$I = F_{pw}\ i^2 = 0.166\ cm^4$$

It is therefore sufficient even if the previously effected approximation had been a little too favorable. On the other hand, a further reduction in inertia moment does not seem advisable unless particular structural reasons make this expedient.

Now it remains to be proved whether the plate wall prior to forming tension wrinkles actually buckles as whole wall, the sheet together with the uprights forming bulges.

Tension wrinkles (buckling between uprights) form when

$$\tau_{k_1} = 7.8\ E \left(\frac{s}{t}\right)^2 = 49\ kg/cm^2$$

The plate wall buckles as a whole (reference 3) when:

$$\tau_{k_2} = \frac{33\ E}{h^2\ s} \sqrt[4]{\left(\frac{J}{t}\right)^3 \frac{s^3}{12}}$$

$$= 17.7\ \frac{E}{h^2\ s} \sqrt[4]{\left(\frac{J\ s}{t}\right)^3} = 269\ \frac{kg}{cm^2}$$

In other words, the buckling load of the whole plate wall is in this case far above the load at which wrinkles are formed. But there are also cases where the buckling load of the entire reinforced wall is lower than that at which tension wrinkles are formed. They occur in the event that the buckling load is only slightly exceeded or that the uprights are very closely spaced so that the inertia moment of the uprights does not become very much higher than the tension-field theory stipulates. In cases of that kind the safety of the entire plate wall against buckling rests with the stiffness of the uprights.

TEST PROCEDURE

The tests were made with the set-up already described in the report on the compression tests, the arrangement for the shear tests being supplemented in a few places. The loading device (fig. 13) served for applying the transverse forces. The transmission being by lever and pulleys, the dynamometer G registered 1/4 of the whole transverse force. Turnbuckle N served to adjust the force. The calibration of this set-up with allowance for any friction showed an accuracy of ±1 percent. To initiate the shear in the dural rails, they were pushed by means of threaded pins A and nuts B (fig. 14) so strongly against the cheeks K that the shearing force could be transmitted by friction.

Two Martens instruments mounted at C (fig. 13), above and below the test specimen, registered the relative shifting of the cheeks. In the determination of the angle of shifting from the readings of the two mirrors, the elastic deformation of the cheeks K due to stresses induced by the loading, were taken into consideration.

The tests, 27 different loading conditions, were made on 0.4, 0.2, and 0.1 mm gage spring-hard brass sheet; that is, three different shear stresses with each one of the three sheet thicknesses, and three different compressive stresses in the duralumin rails for each shearing stress. The number of inclination measurements at each load stage was about the same as in the compression tests, averaging about 600.

INTERPRETATION OF TESTS

The calculation of the mean stresses from the recorded deformations has already been discussed elsewhere (reference 2). But in distinction to the method employed in these (compression) tests restricted to deformation measurements and consequently of secondary importance as regards the size of elasticity modulus, the utilization of the recorded transverse force was necessary in the interpretation of the shear tests. For it was found that the determination of τ from transverse force and sheet thickness was not as reliable as that of the angle of displacement from the records of the mirrors. And this is readily understood from a consideration of the force relations in

the clamping rails. The sheet must always slip a little in these rails and specifically, the width up to which it slips into the clamp is such that the share of the energizing pressure falling to the slipping surface develops enough friction to initiate the shearing force. For that reason the sheet width used for computing the angle of slippage is a somewhat doubtful value and it was therefore always computed from the shearing stress conformable to

$$g = \frac{\tau}{G} - J_{xy}^{xy}$$

The shear modulus was determined from the elasticity modulus, corresponding to $G = E \frac{m}{2(m+1)}$. The transverse contraction factor m was appraised at 10/3; the elasticity modulus was established by tension test.

A repetition of the test data in form of effective width was omitted in the first part of this report because this concept is too involved for actual use on shear-stressed sheets. Nevertheless, the effective width was important for the subsequent evaluation of the tests, since it assures the representation of the results in a specially uniform fashion, which then formed the basis for plotting figure 4. The effective width of sheet-metal walls in shear was defined as follows:

$$b_m = \frac{t}{2} \frac{\sigma_{xz} - \sigma_{xm}}{\sigma_{xz} - \sigma_p}$$

where (the notations are those of the report on the compression tests):

σ_p, is the stress in upright

$\sigma_{xm} = \frac{1}{t} \int_0^t \bar{\sigma}_x \, dy$, mean stress in sheet in the x-direction

σ_{xz}, stress from tension-field theory in x-direction for equal σ_{xp} and τ.

Figure 16 gives the value b_m/t versus $p\tau \left(\frac{t}{s}\right)^2$. Here the factor $p = 1 - 0.86 \frac{\sigma_p}{\tau}$ was empirically so determined that the test points fell all more or less on a curve

despite the unlike σ_p/τ. This curve then served as a basis for figure 4.

The quantities given in the other curves (figs. 5 to 11) were readily established for each load stage from the experimentally defined stress and form-change quantities. Figures 17 to 21 give these curves again with test points included.

Translation by J. Vanier,
National Adviaory Committee
for Aeronautics.

REFERENCES

1. Wagner, Herbert: Flat Sheet Metal Girder with Very Thin Metal Web. Part I: General Theories and Assumptions. T.M. No. 604, N.A.C.A., 1931.

Wagner, Herbert: Flat Sheet Metal Girder with Very Thin Metal Web. Part II: Sheet Metal Girders with Spars Resistant to Bending - Oblique Uprights - Stiffness. T.M. No. 605, N.A.C.A., 1931.

Wagner, Herbert: Flat Sheet Metal Girders with Very Thin Metal Web. Part III: Sheet Metal Girders with Spars Resistant to Bending - The Stress in Uprights - Diagonal Tension Fields. T.M. No. 606, N.A.C.A., 1931.

2. Lahde, R., and Wagner, H.: Luftfahrtforschung, vol. 13, no. 7, (1936), p. 214.

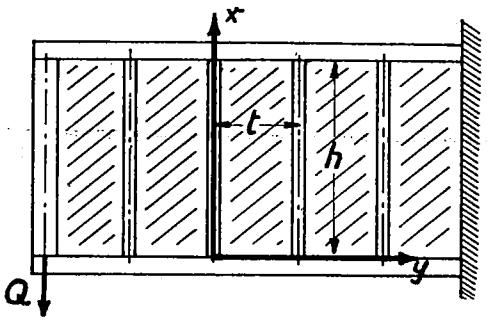

Figure 1.- Plate girder.

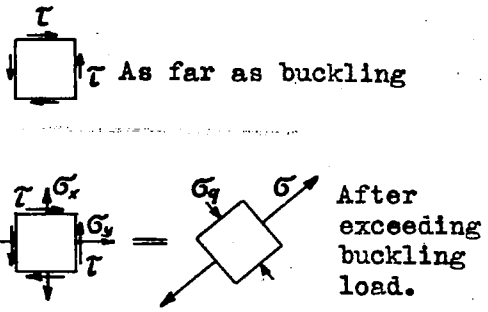

Figure 2.- Stress of web element.

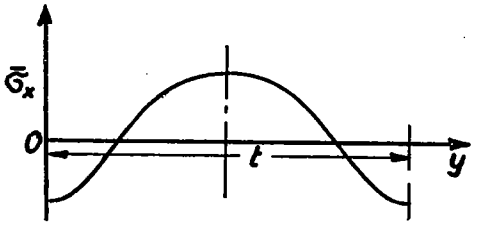

Figure 3.- Distribution of vertical stress component of plate web buckled in shear.

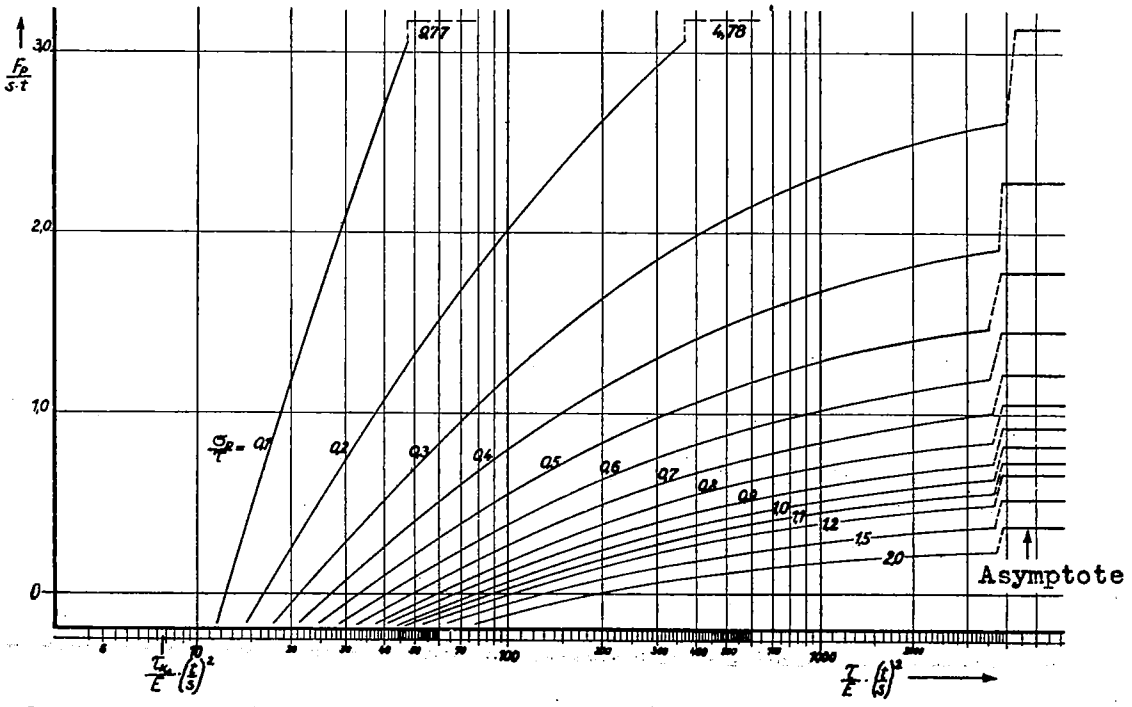

Figure 4.- Ratio of requisite area of upright F_p to relative sheet surface s t, plotted against the degree of exceeded shear-buckling load $\frac{\tau}{E}\left(\frac{t}{s}\right)^2$ for different ratios of compression σ_p in upright to shearing stress τ.

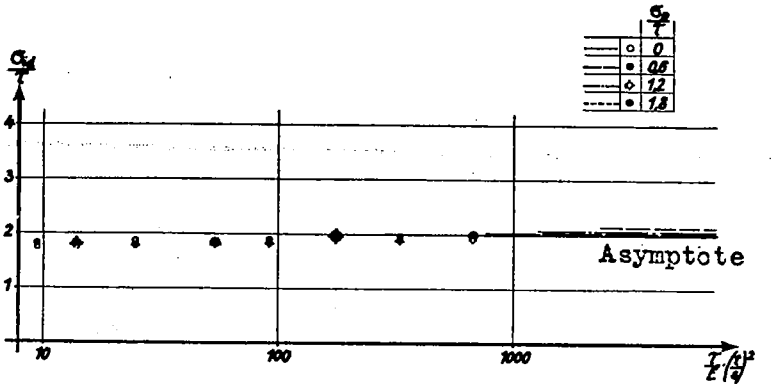

Figure 5.- Stress in neutral axis of sheet measured midway between two uprights.

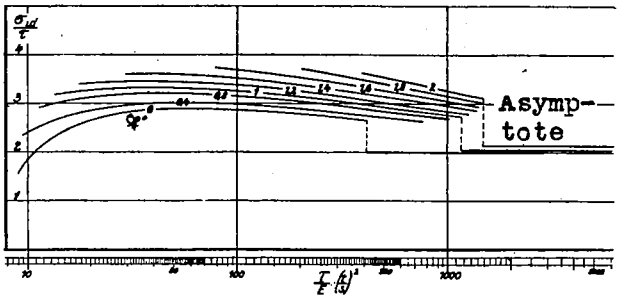

Figure 6.- Stress of outside fiber of sheet measured midway between two uprights.

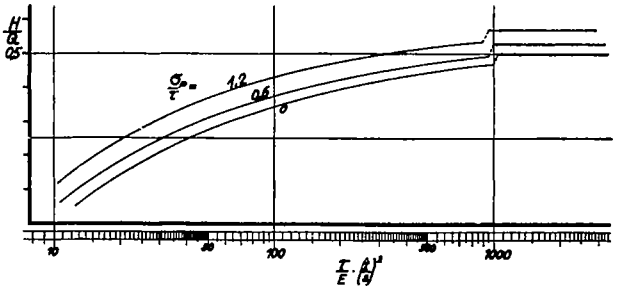

Figure 7.- Ratio of cumulative longitudinal force H produced in a flange to total transverse force Q.

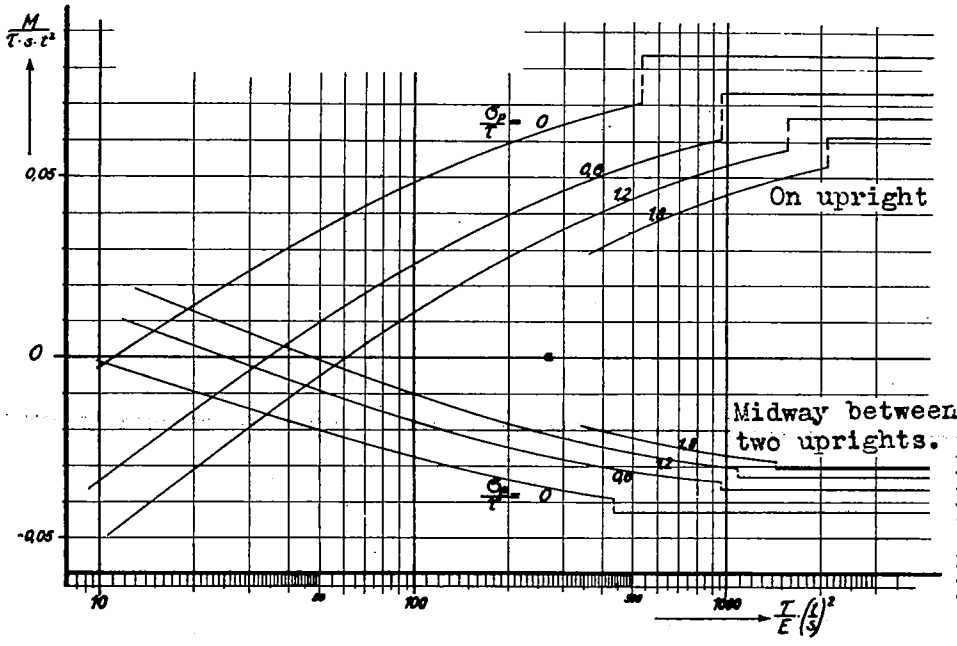

Figure 8.- Maximum bending moments M in the flanges.

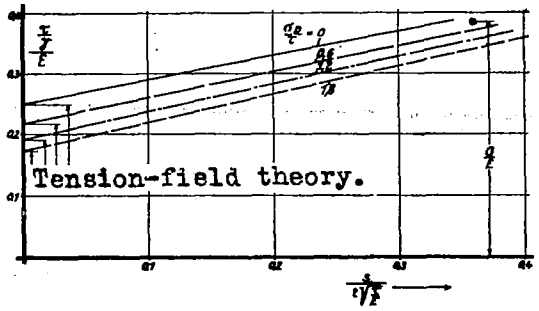

Figure 9.- Angle of displacement τ/γ substitutes for G in the particular formula for the angle of displcement.

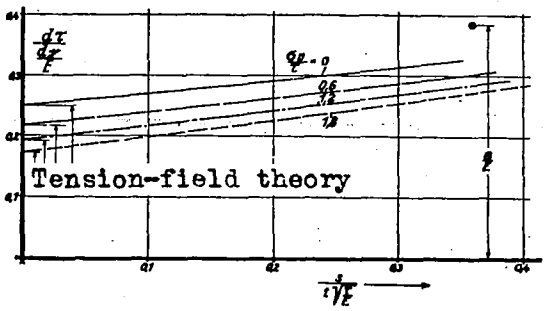

Figure 10.- Stiffness in shear, $\delta_\tau/\delta_\gamma$ substitutes for shear modulus G in the shear stiffness formula.

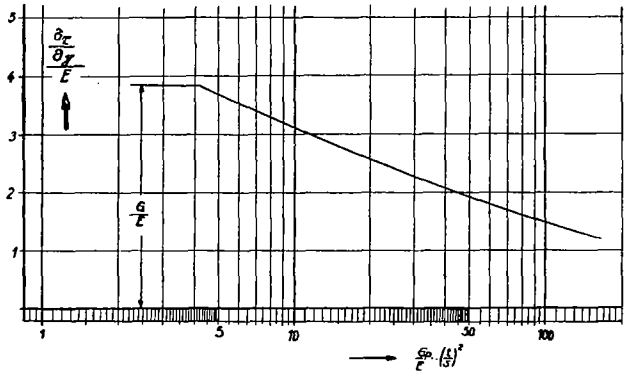

Figure 11.- Shear stiffness in plate walls made to buckle under compressive stresses σ_p applied only in direction of the long edges.

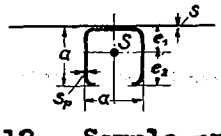

Figure 12.- Sample problem, U section with
$e_1 + e_2 = a = 2.5\,i$; $e_1 = i$
$F_p = 3.5\,a\,s_p$.
i = inertia radius

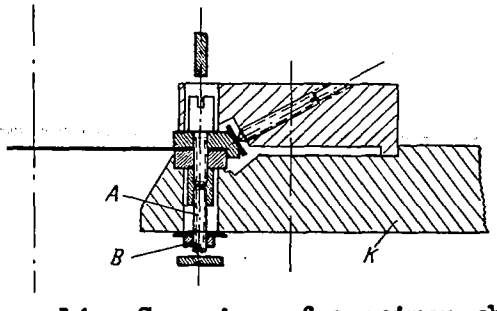

Figure 14.- Securing of specimen sheet.

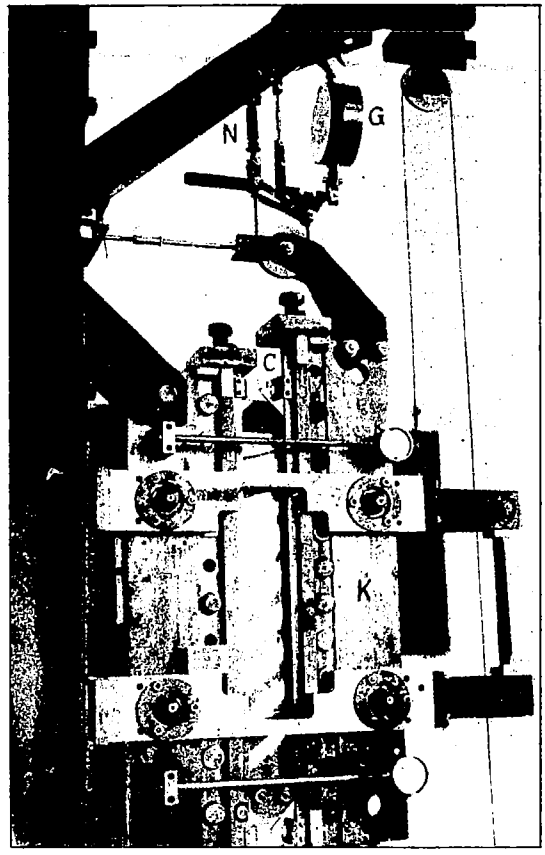

Figure 13.- Experimental arrangement.

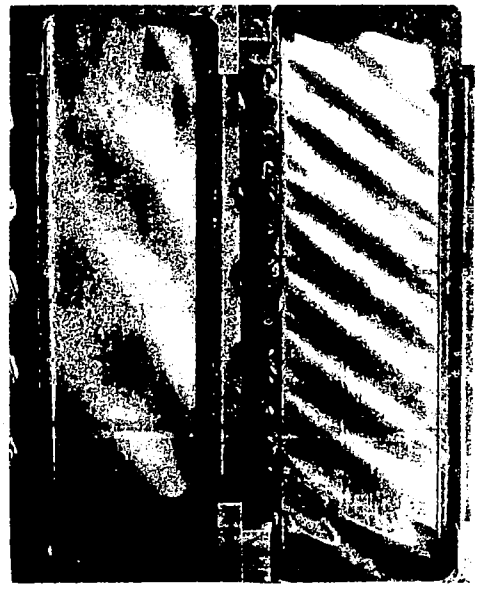

Figure 15.- Wrinkling observed when the shear-buckling load was a, little; b, much exceeded.

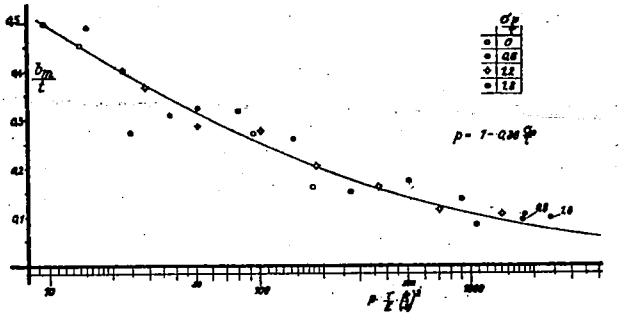

Figure 16.- Effective width in shear, two uprights.

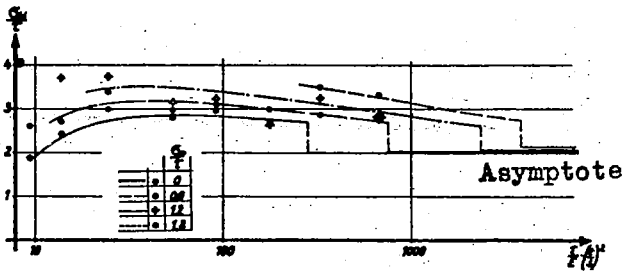

Figure 17.- Stress of outside fiber of sheet midway between

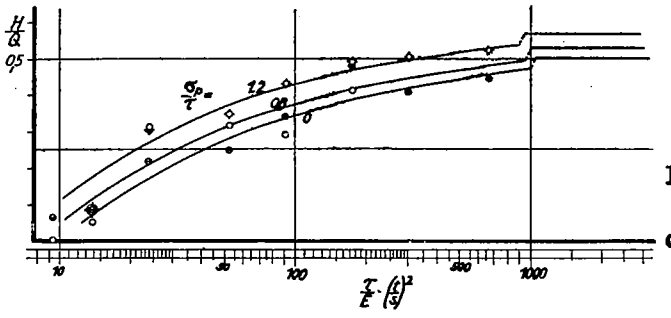

Figure 18.- Cumulative stress H in each flange due to sheet tension.

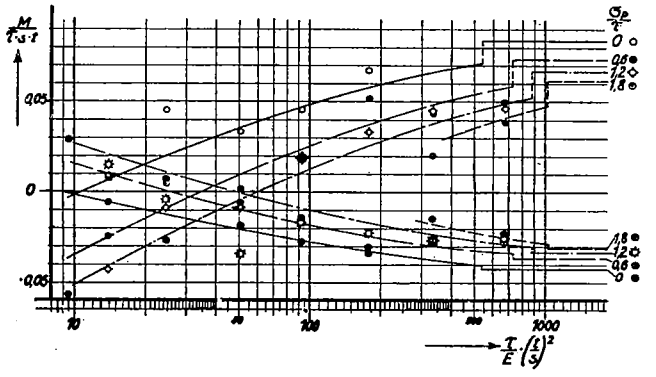

Figure 19.- Flange bending moments.

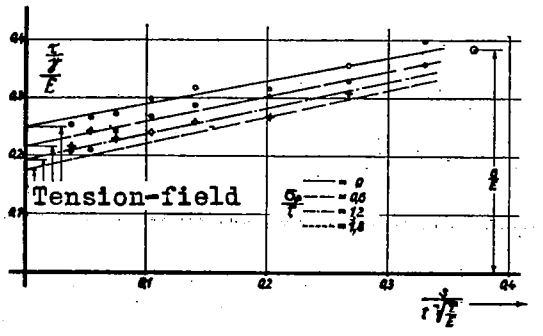

Figure 20.- Angle of displacement.

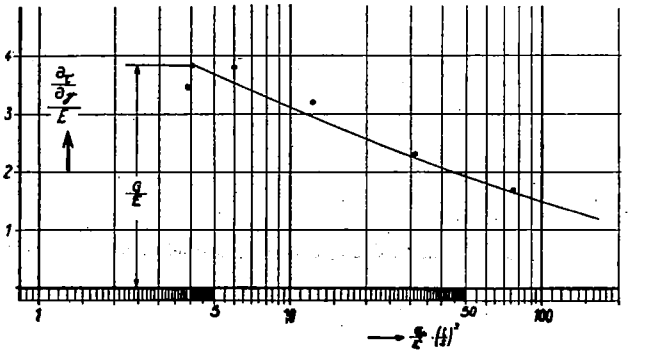

Figure 21.- Shear stiffness of sheets buckled under compressive stresses σ_p only.